SEMI-ANNUAL REPORT

State of Stress in the Rupture Zone of Large Earthquakes

Grant No. 14-08-0001-G1773

1 December 1990 - 31 May 1991

Hiroo Kanamori
Seismological Laboratory, California Institute of Technology
Pasadena, California (818) 356-6914

Investigation

The 1990 Rudbar-Manjil earthquake, Iran.

Results

The June 1990 Rudbar earthquake is remarkable in that it was a major strike-slip event in a region which is dominated by thrust faults and in which thrusting has been found to be the predominant mode of seismicity. The surface fault has been mapped by Berberian et al. (1991), and consists of three very steeply dipping en-echelon fault strands with ESE strike. The total length of the surface fault amounts to 80 kilometers. The length of the individual segments and the amount of displacement increase from the WNW to the ESE. Remarkably, there was a vertical displacement of up to a meter with the southside uplifted as opposed to a left-lateral displacement of only 60 centimeters. This is at odds with the seismic observations which indicate pure left-lateral strike-slip. Also, the fault that ruptured did not have any evidence for previous activity contrary to nearby faults.

1. Body-wave analysis

The waveforms at teleseismic distances look quite complex indicating that the rupture consisted of several subevents. The records from various stations for this earthquakes show that the rupture started off with a small subevent and that the energy release increases towards the end of the rupture. The initial NEIC location for this event was off by about 100 kilometers which may be due to misidentification of first arrivals because of the very emergent onset of the records.

The body-wave inversion method used here has been described in detail in Kikuchi and Kanamori (1991). It solves for the spatial and temporal distribution of subevents as well as for their mechanism by iteration. In this particular inversion the subevents were constrained along a fault segment with a strike of 110 degrees and a vertical fault plane. We used eight nodes along the fault with a separation of 15 kilometers. The depth of the subevents were constrained initially between 5 and 25 kilometers with a separation of 5 kilometers but on the basis of these earlier inversion runs we constrained the depths between 7.5 and 17.5 kilometers. The only constraint on the mechanism of the subevents was a double co uple constraint. Because of the gradual build-up of energy release we had to impose a time window for the first subevent to occur, but even then, the very first beginning of the rupture remains unsolved. The subevent distribution is given in Figure 1 with the corresponding subevents given in Table 1, and it is clear that the largest energy release occurred in the SE part of the fault zone. In order to explain the data we need at least four subevents which are all strike-slip but with slight variations in strike. Because of the strike-slip mechanism we have several stations which are close to a nodal plane and therefore their waveforms are very sensitive to small changes in focal plane parameters. We therefore think that these variations in strike are significant. The locations of the subevents and their sizes agree well with the surface observations (Berberian et al., 1991). There is however no evidence for any significant vertical movement.

The results from our CMT inversion using long-period surface waves agree quite well with the body-wave results apart from the dipping secondary fault plane.

2. Discussion

When we compare the results from our body-wave inversion and the observations on the surface rupture we can see that there is generally good agreement between the two. The increase in moment release towards the east matches the increased fault length and offset. This and the variation in strike between the different subevents suggest that the observed segmentation of the fault extends to the depth at which most of the seismic energy was released. The segmentation on the surface, called Riedel faulting, has been studied extensively in sand-box (Naylor et al. 1986) and in the field (e.g. Harding, 1973). Riedel faulting is generally associated with a buried wrench fault which imposes movement on the overburden. This particular Riedel pattern, generally designated 'R' or synthetic Riedel, is characteristic for faults with a very low strain rate or faults in their early stages of development. We may therefore expect this kind of source complexity for faults in their early stages.

References

Berberian, M., Qorashi, M., Jackson, J. A., Priestly, K., Wallace, T., 1991. The Rudbar-Tarom earthquake of 20 June 1990 in NW Persia: preliminary field and seismological observations, and its tectonic significance. In prep.

Harding, T. P., 1973. Newport-Inglewood Trend, California - an example of wrenching style deformation. AAPG bull., 57(1), 97-116.

Kikuchi, M., Kanamori, H., 1991. Inversion of complex body-waves III. In press.

Naylor, M. A., Mandl, G., Sijpestein, C.H.K., 1986. Fault geometries in basement-induced wrench faulting under different initial stress states. J.Struct.Geol., 7 (8), 737-752.

Table 1

sub-event	time after JB	depth	Moment, 10^{25} dyne-cm	strike	dip	slip
1	4.0	12.5	8.73	281.5	73.7	1.8
2	7.0	15.0	10.40	297.1	70.8	7.1
3	17.5	10.0	46.53	295.5	81.2	1.5
4	25.0	7.5	24.78	130.7	80.6	-3.8
Total			84.89	298.5	84.1	1.3
CMT			120.	117.4	89.5	-26.5

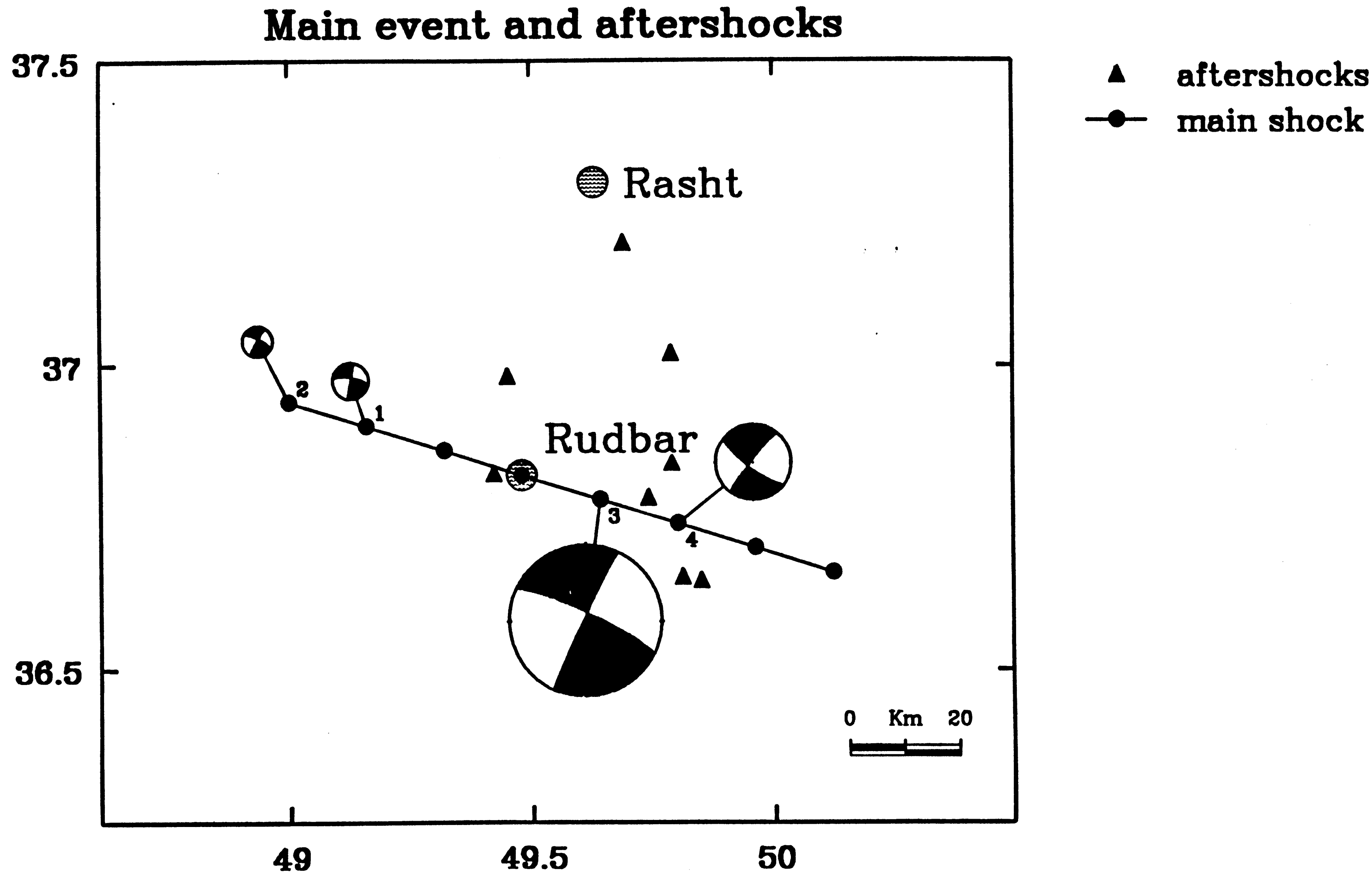
Main event and aftershocks
37.5
37
36.5
49
49.5
50
Rasht
Rudbar
1
2
3
4
0 Km 20
aftershocks
main shock

Figure 1